

LDA + U Calculation of Electronic and Thermoelectric Properties of Doped Tetrahedrite $\text{Cu}_{12}\text{Sb}_4\text{S}_{13}$

K. KNÍŽEK ^{1,2}, P. LEVINSKÝ,¹ and J. HEJTMÁNEK¹

1.—Institute of Physics of the CAS, Cukrovarnická 10, 162 00 Prague 6, Czech Republic.
2.—e-mail: knizek@fzu.cz

Tetrahedrite-based thermoelectric materials have received much attention in recent years due to their good thermoelectric performance and earth-abundance. The parent compound $\text{Cu}_{12}\text{Sb}_4\text{S}_{13}$ exhibits a high power factor and low lattice thermal conductivity. Further enhancement of the thermoelectric figure of merit ZT is expected in substituted compounds, primarily at the Cu site $\text{Cu}_{12-x}\text{M}_x\text{Sb}_4\text{S}_{13}$. In this work we have studied the impact of substitution effects on thermoelectric properties using density-functional theory electronic structure calculations in combination with calculation of electrical transport properties by the BoltzTrap program.

Key words: Tetrahedrites, thermoelectric, DFT, BoltzTrap

INTRODUCTION

Direct conversion of thermal to electric energy using thermoelectric modules represents a prospective method for recovery of the high temperature waste heat. The energy conversion efficiency of the thermoelectric device is determined by the Carnot efficiency and by the dimensionless figure of merit (ZT) of the thermoelectric material $ZT = T(S^2 \cdot \sigma) / (\kappa_e + \kappa_p)$, where S is the thermoelectric power or Seebeck coefficient, σ is the electrical conductivity, κ_e and κ_p are the electronic and phononic parts of the thermal conductivity, and T is the absolute temperature. In order to characterize the electrical properties separately, the power factor $P = S^2 \cdot \sigma$ is also defined.

Among other thermoelectric materials, tetrahedrites with the basic formula $\text{Cu}_{12}\text{Sb}_4\text{S}_{13}$ are promising p -type thermoelectric materials due to their high power factor and extremely low lattice thermal conductivity.¹ The promising thermoelectric properties can be related to their complex crystal structure consisting of 58 atoms per unit cell.² The important advantage of tetrahedrites, in

comparison to ‘classical’ thermoelectric materials like Bi_2Te_3 , is that they basically consist of earth-abundant and environmentally-friendly elements. Using a simple ionic picture, the formula can be written as $\text{Cu}_{10}^+\text{Cu}_2^+\text{Sb}_4^{3+}\text{S}_{13}^{2-}$, where the Cu^{2+} cations are typically replaced by other divalent transition metals like Mn, Fe, Co, Ni or Zn^{3–10} or p -block elements like Cd or Sn.^{11,12}

It was recently demonstrated that also the s -block element, namely Mg^{2+} , could be successfully substituted for Cu^{2+} .¹³ In this paper, we have attempted a study of the electronic structure of Mg-substituted tetrahedrite in comparison with a series of tetrahedrites substituted by other elements at Cu-site $\text{Cu}_{12-x}\text{M}_x\text{Sb}_4\text{S}_{13}$ with a similar level of doping. The electronic structure was studied using a combination of Wien2k program based on DFT method¹⁴ and the BoltzTrap package based on the Boltzmann transport theory.¹⁵ It was previously shown, that the bands crossing the Fermi level are mainly composed by Cu d -orbitals.^{6,16,17} Therefore, in order to assess the substitution effect of a similar level of doping, we have selected for the electronic structure calculation tetrahedrites with substitution of Cu by Zn ($\text{Cu}_{11}\text{ZnSb}_4\text{S}_{13}$), Mg ($\text{Cu}_{11}\text{MgSb}_4\text{S}_{13}$) and vacancy ($\text{Cu}_9\text{Zn}_2\text{Sb}_4\text{S}_{13}$) with a similar level of d -band filling ~ 9.9 as the parent compound $\text{Cu}_{12}\text{Sb}_4\text{S}_{13}$.

METHODS OF CALCULATIONS

The calculations were made with the WIEN2k program.¹⁴ This program is based on the density-functional theory (DFT) and uses the full-potential linearized augmented plane-wave (FP LAPW) method with the dual basis set. In the LAPW methods, the space is divided into atomic spheres and the interstitial region. The electron states are then classified as the core states that are fully contained in the atomic spheres and the valence states. The core states were defined as an electronic configuration (Ne 3s²) for Cu and Zn, as (He) for Mg, as (Ne) for S, and as (Kr) for Sb atoms. The radii of the atomic spheres were taken as 2.2 a.u. for Cu and the atoms substituted at the Cu position, i.e., Zn and Mg, 1.9 a.u. for S and 2.2 a.u. for Sb. The number of *k*-points in the irreducible part of the Brillouin zone was 64. All calculations were spin-polarized.

To improve the description of 3*d* electrons, we used the LDA+U method. In this method, an orbitally dependent potential is introduced for the chosen set of electron states, i.e., for 3*d* states in our case. This additional potential has an atomic Hartree–Fock form but with screened Coulomb and exchange interaction parameters. The fully localized limit version of the LDA+U method was employed. The parameters $U = 4$ eV and $J = 1$ eV were used.

The calculations of the electrical transport properties were done within Boltzmann transport theory using the BoltzTrap package¹⁵ under the constant relaxation time approximation for the charge carriers. The formulas used in calculation for Seebeck coefficient (S), electrical conductivity (σ) and the electronic part of thermal conductivity (κ_e), have a general form:

$$\sigma_{ij} = K_{ij}^0, \quad (1)$$

$$S_{ij} = \frac{1}{eT} K_{ij}^1 / K_{ii}^0, \quad (2)$$

$$\kappa_{ij}^e = \frac{1}{e^2 T} K_{ij}^2, \quad (3)$$

where $K_{\alpha\beta}^n(T, \mu)$ is

$$K_{\alpha\beta}^n = \int \frac{\tau e^2}{\hbar^2} \frac{\partial \epsilon}{\partial \mathbf{k}_\alpha} \frac{\partial \epsilon}{\partial \mathbf{k}_\beta} (\epsilon - \mu)^n \left[-\frac{\partial f_\mu(T, \epsilon)}{\partial \epsilon} \right] d\epsilon, \quad (4)$$

where μ is the chemical potential, ϵ is an energy variable, T is the absolute temperature, e is the electron charge and τ is a relaxation time. The main weight in the above mentioned integration have partially occupied states over the characteristic energy $\mu \pm 3kT$, which is approximately ± 75 meV around the chemical potential at 300 K and approximately ± 200 meV at 800 K.

RESULTS AND DISCUSSION

The tetrahedrite Cu₁₂Sb₄S₁₃ crystallizes in a cubic space group $I\bar{4}3m$. Copper cations occupy the structure in two kinds of crystallographic sites, either tetrahedrally coordinated by S anions (further denoted as Cu4) or trigonally coordinated by S (Cu3), each with multiplicity 12. In order to make possible a partial substitution at the Cu sites, the symmetry of the structure has been lowered to $P\bar{4}$, so that each Cu site has been split into four sites with multiplicities 2 and 4. The Cu atom in the sites with multiplicity 2 were then substituted by the selected atoms in order to adjust the *d*-band filling ~ 9.9 . The atomic positions were optimized by force minimization during calculation. Substitution at both the Cu3 and Cu4 sites were compared for all the substituted compounds, in all cases the substitution at the Cu4 sites resulted in lower total energy.

The calculated density of states (DOS) are displayed in Fig. 1. All the calculations were started as spin-polarized. The electronic structure of the parent compound Cu₁₂Sb₄S₁₃ converged to a non-magnetic solution, whereas the calculations of the substituted compounds resulted in a spin-polarized type of DOS at the Fermi level. The states near the Fermi level are mainly composed of antibonding states of Cu4 and S, whereas the contribution of Cu3 is smaller. The states of the substituted atoms Zn and Mg are far from the Fermi level, so their substitution does not directly modify the DOS at E_F . Nevertheless, since they replace the Cu4 cations, they modulate the Cu4-S bonding in their vicinity and thus indirectly influence the DOS at E_F .

In order to separate from the thermoelectric figure of merit ZT the terms which can be calculated by the BoltzTrap program, the formula can be rewritten as follows^{18,19}

$$ZT = T \frac{S^2 \sigma / \tau_e}{\kappa_e / \tau_e} \cdot \frac{\kappa_e}{\kappa_e + \kappa_p} = ZT_{el} \cdot \frac{\kappa_e}{\kappa_e + \kappa_p}, \quad (5)$$

where the parameters of first term can be calculated by BoltzTrap, namely Seebeck (S), electrical conductivity divided by relaxation time of electrons (σ / τ_e) and the electronic part of the thermal conductivity divided by relaxation time of electrons (κ_e / τ_e). The second term includes the phononic part of the thermal conductivity (κ_p) in combination with κ_e where the relaxation time of electrons (τ_e) is not canceled out. The term ZT_{el} can be considered as the maximal ZT if $\kappa_p = 0$. In that case the second term is equal to 1 and $ZT = ZT_{el}$. As soon as $\kappa_p > 0$, the second term becomes less than 1 and ZT diminishes proportionally.

The expression for ZT_{el} can be simplified with the help of the Wiedeman–Franz law, which quantifies the relation of the electron part of thermal conductivity and electrical conductivity as

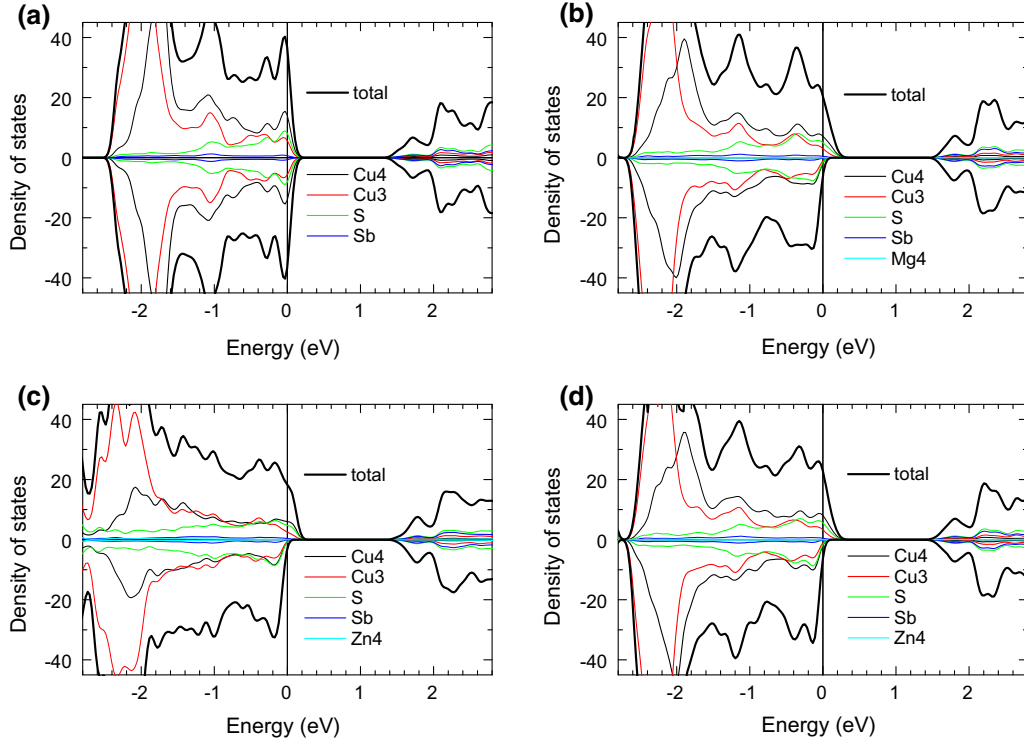


Fig. 1. Calculated total and partial density of states (DOS) of (a) $\text{Cu}_{12}\text{Sb}_4\text{S}_{13}$, (b) $\text{Cu}_{11}\text{MgSb}_4\text{S}_{13}$, (c) $\text{Cu}_9\text{Zn}_2\text{Sb}_4\text{S}_{13}$ and (d) $\text{Cu}_{11}\text{ZnSb}_4\text{S}_{13}$ (Color figure online).

$$L = \frac{\kappa_e}{T\sigma} = \frac{\pi^2 k_B^2}{3 e^2}, \quad (6)$$

where L is the Lorenz number, which for materials with degenerate charge carriers, approaches the constant value $L_{WF} = 2.44 \times 10^{-8} \text{ V}^2\text{K}^{-2}$. Substituting this relation into an expression for ZT_{el} we obtain¹⁸

$$ZT_{el} = T \frac{S^2 \sigma / \tau_e}{LT \sigma / \tau_e} = \frac{S^2}{L}. \quad (7)$$

Apparently, ZT_{el} should only depend on S^2 in ideal systems with degenerate charge carriers. Nevertheless, deviations from Wiedeman–Franz law in dependence on temperature is commonly observed, in particular in materials with correlated electrons.

Based on the above assumptions, we have calculated the Seebeck coefficient S , the Lorenz number as the ratio of the electron part of thermal conductivity κ_e and the electrical conductivity σ , and the resulting ZT_{el} for the studied series of tetrahedrites using the BoltzTrap program, see Fig. 2. The calculated Seebeck coefficient is the highest for $\text{Cu}_9\text{Zn}_2\text{Sb}_4\text{S}_{13}$, and for $\text{Cu}_{11}\text{MgSb}_4\text{S}_{13}$ and $\text{Cu}_{11}\text{ZnSb}_4\text{S}_{13}$ is also enhanced compared to $\text{Cu}_{12}\text{Sb}_4\text{S}_{13}$, see the middle panel of Fig. 2.

A comparison of the total DOS focused on the states just near the Fermi level is displayed in Fig. 3. The main weight of states included in the thermoelectric properties calculations is limited to the energy range about $\pm 3k_B T$, which is approximately

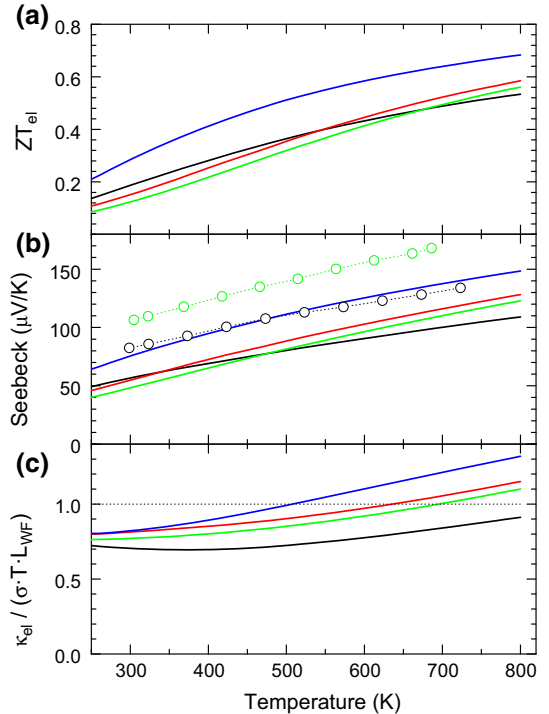


Fig. 2. (a) ZT_{el} (see Eq. 5), (b) Seebeck coefficient, and (c) the ratio of the electron part of thermal conductivity κ_e and the electrical conductivity σ normalized to Lorenz number for degenerate carriers L_{WF} , calculated by the BoltzTrap program using band structure obtained by a LDA+U calculation. (black line) $\text{Cu}_{12}\text{Sb}_4\text{S}_{13}$, (red line) $\text{Cu}_{11}\text{ZnSb}_4\text{S}_{13}$, (green line) $\text{Cu}_{11}\text{MgSb}_4\text{S}_{13}$ and (blue line) $\text{Cu}_9\text{Zn}_2\text{Sb}_4\text{S}_{13}$. The experimental Seebeck coefficients of (black circle) $\text{Cu}_{12}\text{Sb}_4\text{S}_{13}$ and (green circle) $\text{Cu}_{11.25}\text{Mg}_{0.75}\text{Sb}_4\text{S}_{13}$ are also displayed in (b) (Color figure online).

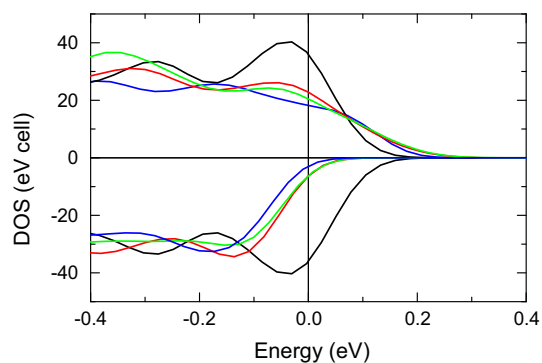


Fig. 3. Comparison of the calculated total DOS near the Fermi level of (black line) Cu₁₂Sb₄S₁₃, (red line) Cu₁₁ZnSb₄S₁₃, (green line) Cu₁₁MgSb₄S₁₃, (blue line) Cu₉Zn₂Sb₄S₁₃ (Color figure online).

± 80 meV around the Fermi level at 300 K and approximately ± 200 meV at 800 K. It can be seen, that DOS within this energy range of Cu₉Zn₂Sb₄S₁₃ is increasing with lowering energy with maximum around -200 meV, whereas DOS of the other compounds have a maximum closer to the Fermi level around -50 meV. This difference is reflected in the calculated Seebeck coefficient, which is the highest for Cu₉Zn₂Sb₄S₁₃.

The comparison with the experimental data of Cu₁₂Sb₄S₁₃ and Mg-substituted ($x = 0.75$ as determined by EDX) samples revealed, that the calculated Seebeck coefficient is lower than the observed one for both compounds, nevertheless, there is an agreement as regards the trend of increasing Seebeck upon substitution.¹³ A similar trend is also observed in the case of the Lorenz number, canceling thus partially the contribution of Seebeck to ZT_{el} . Nevertheless, the contribution of S^2 to the ZT_{el} was found to be decisive in the case of Cu₉Zn₂Sb₄S₁₃, which exhibits also the highest ZT_{el} , whereas for the compounds with Mg and Zn substitution, the enhancement of S^2 and L approximately cancels, and the resulting ZT_{el} is comparable to that of Cu₁₂Sb₄S₁₃.

CONCLUSIONS

We have studied the electronic structure and the thermoelectric properties of the series of tetrahedrites Cu_{12-x}M_xSb₄S₁₃ substituted at Cu4 site (Cu in tetrahedron) with similar level of d -band filling ~ 9.9 as the parent compound Cu₁₂Sb₄S₁₃. In order to partially characterize the thermoelectric properties within the frame of Boltzmann transport theory (BoltzTrap program), we have calculated the electronic part ZT_{el} of the thermoelectric figure of merit ZT , which includes the Seebeck coefficient and the ratio of the electron part of thermal conductivity to the electrical conductivity (Lorenz number). The Seebeck coefficient calculated using the BoltzTrap

program is positive for all the studied compounds. The highest Seebeck coefficient was determined for Cu₉Zn₂Sb₄S₁₃. Seebeck coefficients of Cu₁₁ZnSb₄S₁₃ and Cu₁₁MgSb₄S₁₃ are similar and also enhanced compared to Cu₁₂Sb₄S₁₃. Cu₉Zn₂Sb₄S₁₃ also exhibits the highest ZT_{el} , whereas the resulting ZT_{el} of tetrahedrites with Mg and Zn substitution is comparable to that of Cu₁₂Sb₄S₁₃.

ACKNOWLEDGMENTS

This work was supported by the Project No. 18-12761S of the Czech Science Foundation. Access to computing and storage facilities owned by parties and projects contributing to the National Grid Infrastructure MetaCentrum provided under the programme “Projects of Large Research, Development, and Innovations Infrastructures” (CESNET LM2015042), is greatly appreciated.

REFERENCES

1. X. Lu, D.T. Morelli, Y. Xia, F. Zhou, V. Ozolins, H. Chi, X.Y. Zhou, and C. Uher, *Adv. Energy Mater.* 3, 342 (2013).
2. R. Chetty, A. Bali, and R.C. Mallik, *J. Mater. Chem. C* 3, 12364 (2015).
3. K. Suekuni, K. Tsuruta, T. Ariga, and M. Koyano, *Appl. Phys. Express* 5, 51201 (2012).
4. K. Suekuni, K. Tsuruta, M. Kunii, H. Nishiata, E. Nishibori, S. Maki, M. Ohta, A. Yamamoto, and M. Koyano, *J. Appl. Phys.* 113, 43712 (2013).
5. J. Heo, G. Laurita, S. Muir, M.A. Subramanian, and D.A. Keszler, *Chem. Mater.* 26, 2047 (2014).
6. K. Suekuni, Y. Tomizawa, T. Ozaki, and M. Koyano, *J. Appl. Phys.* 115, 143702 (2014).
7. X. Lu, D.T. Morelli, Y. Xia, and V. Ozolins, *Chem. Mater.* 27, 408 (2015).
8. R. Chetty, D.S.P. Kumar, G. Rogl, P. Rogl, E. Bauer, H. Michor, S. Suwas, S. Puchegger, G. Giester, and R.C. Mallik, *Phys. Chem. Chem. Phys.* 17, 1716 (2015).
9. R. Chetty, A. Bali, M.H. Naik, G. Rogl, P. Rogl, M. Jain, S. Suwas, and R.C. Mallik, *Acta Mater.* 100, 266 (2015).
10. S. Tippireddy, R. Chetty, M.H. Naik, M. Jain, K. Chattopadhyay, and R.C. Mallik, *J. Phys. Chem. C* 122, 8735 (2018).
11. D.S.P. Kumar, R. Chetty, P. Rogl, G. Rogl, E. Bauer, P. Malar, and R.C. Mallik, *Intermetallics* 78, 21 (2016).
12. Y. Kosaka, K. Suekuni, K. Hashikuni, Y. Bouyrie, M. Ohta, and T. Takabatake, *Phys. Chem. Chem. Phys.* 19, 8874 (2017).
13. P. Levinský, C. Candolfi, A. Dauscher, B. Lenoir, and J. Hejtmanek, *J. Electron. Mater.* (accepted).
14. P. Blaha, K. Schwarz, G. K. H. Madsen, D. Kvasnicka, and J. Luitz, WIEN2k, An Augmented Plane Wave + Local Orbitals Program for Calculating Crystal Properties. Technische Universität, Wien (2014). www.wien2k.at.
15. G.K.H. Madsen and D.J. Singh, *Comput. Phys. Commun.* 175, 67 (2006).
16. Y. Bouyrie, C. Candolfi, V. Ohorodniichuk, B. Malaman, A. Dauscher, J. Tobola, and B. Lenoir, *J. Mater. Chem. C* 3, 10476 (2015).
17. X. Lu, W. Yao, G.W. Wang, X.Y. Zhou, D. Morelli, Y.S. Zhang, H. Chi, S. Hui, and C. Uher, *J. Mater. Chem. A* 4, 17096 (2016).
18. Y.O. Ciftci and S.D. Mahanti, *J. Appl. Phys.* 119, 145703 (2016).
19. M. Miyata, T. Ozaki, T. Takeuchi, S. Nishino, M. Inukai, and M. Koyano, *J. Electron. Mater.* 47, 3254 (2018).